



Riluzole prodrugs for melanoma and ALS: Design, synthesis, and in vitro metabolic profiling

Mark E. McDonnell^a, Matthew D. Vera^a, Benjamin E. Blass^a, Jeffrey C. Pelletier^a, Richard C. King^b, Carmen Fernandez-Metzler^b, Garry R. Smith^a, Jay Wrobel^a, Suzie Chen^c, Brian A. Wall^c, Allen B. Reitz^{a,*}

^a Fox Chase Chemical Diversity Center, Inc., 3805 Old Easton Road, Doylestown, PA 18902, USA

^b PharmaCadence Analytical Services, LLC, 2880 Bergey Road, Suite AA, Hatfield, PA 19440, USA

^c Department of Chemical Biology, Ernest Mario School of Pharmacy, 164 Frelinghuysen Road, Rutgers University, Piscataway, NJ 08854, USA

ARTICLE INFO

Article history:

Received 31 May 2012

Revised 27 June 2012

Accepted 4 July 2012

Available online 21 July 2012

Keywords:

Riluzole

Prodrug

Cancer

Melanoma

Cyp1A2

ABSTRACT

Riluzole (**1**) is an approved therapeutic for the treatment of ALS and has also demonstrated anti-melanoma activity in metabotropic glutamate GRM1 positive cell lines, a mouse xenograft assay and human clinical trials. Highly variable drug exposure following oral administration among patients, likely due to variable first pass effects from heterogeneous CYP1A2 expression, hinders its clinical use. In an effort to mitigate effects of this clearance pathway and uniformly administer riluzole at efficacious exposure levels, several classes of prodrugs of riluzole were designed, synthesized, and evaluated in multiple in vitro stability assays to predict in vivo drug levels. The optimal prodrug would possess the following profile: stability while transiting the digestive system, stability towards first pass metabolism, and metabolic lability in the plasma releasing riluzole. (S)-O-Benzyl serine derivative **9** was identified as the most promising therapeutically acceptable prodrug.

© 2012 Elsevier Ltd. All rights reserved.

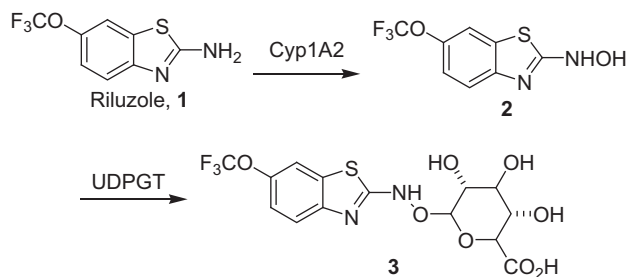
1. Introduction

The glutamatergic system plays a key role in tumor biology.^{1–7} The growth inhibition of various human tumors including colon adenocarcinomas, breast, gliomas, and lung carcinomas by specific antagonists to ionotropic glutamate receptors has been reported.^{2,6} Furthermore, implanted glioma cells with high levels of glutamate release showed a distinct growth advantage.² We have evaluated riluzole (**1**; Scheme 1), the only currently FDA-approved drug for the treatment of amyotrophic lateral sclerosis (ALS),⁸ for potential anti-cancer activity, as it inhibits glutamate release, thus lowering the potential for glutamatergic system signaling and function.^{9,10}

Riluzole blocks the release of glutamic acid and thus lessens the response mediated by the metabotropic glutamate receptor GRM1 (mGluR1) among other receptors that recognize glutamic acid as a cognate ligand. We have shown a reduction in the number of viable cells after treatment with riluzole in two different GRM1-positive melanoma cell lines (C8161 and SKMEL187) while two different GRM1-negative human melanoma cell lines (UACC930 and C81-61) or normal human melanocytes (HEM) were much less sensitive under similar conditions.¹¹ Furthermore, we have also demonstrated a correlation between a decrease in levels of released glutamate and number of viable cells in riluzole-treated C8161

cells.¹¹ These results support the notion that high glutamate release may promote tumor cell growth.^{1–7}

Metastatic melanoma has few treatment options. Surgical resection is the primary modality for cutaneous malignant melanoma but results in local recurrence rates as high as 50%. For a long time the therapeutic standard of care was dacarbazine, a highly cytotoxic drug with severe side effects including vomiting, headache and hair loss.^{12,13} Treatment with dacarbazine has a median progression-free enhancement of survival time of only 1.5 months. Recently, two new drugs showed survival benefit in randomized phase III clinical trials. Ipilimumab, a human monoclonal anti-immunosuppressive antibody against the immune check-point CTLA-4 inhibitory receptor enhanced life expectancy and vemurafenib, a small molecule inhibiting mutated BRAF, improved



Scheme 1. Riluzole (**1**), and metabolites **2** and **3**.

* Corresponding author. Tel.: +1 215 589 6435; fax: +1 215 589 6335.

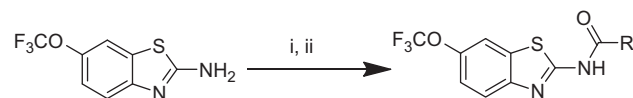
E-mail address: AReitz@fc-cdci.com (A.B. Reitz).

overall survival for several months in most melanoma patients with mutated BRAF.^{14,15} Despite these advances, the clinical responses are not durable and relapse of melanoma is a near-certainty. There is a need for new melanoma treatments that are both disease-modifying and effective in treating patients that are refractory to current treatments. Riluzole, a generally non-toxic drug for which there is significant clinical data available, is the only FDA-approved treatment for ALS.¹⁶ We tested the efficacy of riluzole in melanoma patients with a poor prognosis and severely limited treatment options.¹⁷ Riluzole demonstrated efficacy in this patient group in recently completed phase 0 and phase 2 clinical trials.¹⁷ These results, along with the mild side-effect profile that riluzole has shown among ALS patients, suggests this drug has significant potential for use as an improved treatment for metastatic melanoma.

The clinical use of riluzole is characterized by extensive hepatic metabolism and an exceptionally high level of patient-to-patient variability in drug exposure, due to variable first pass elimination effects caused by heterogeneous expression of the cytochrome P450 isoform CYP1A2.^{18–21} N-Hydroxylation of riluzole by CYP1A2 to give **2** is quickly followed by O-glucuronidation to **3** and subsequent elimination (Scheme 1).²¹ In order to circumvent the first pass metabolism by CYP1A2 we devised a prodrug approach where the riluzole exocyclic nitrogen is masked in such a way as not to be recognized by CYP1A2 as a substrate for oxidation. A successful prodrug would be stable in the gastrointestinal (GI) tract upon oral administration, stable to first pass hepatic metabolism and then cleaved in plasma or at the target tissue to liberate riluzole. Herein we report the identification and selection of a riluzole prodrug suitable for in vivo testing based on the design, synthesis, and rapid in vitro evaluation of the 23 potential riluzole prodrugs shown in Figure 1.

2. Results and discussion

The preparation of prodrugs from amine-containing drugs and drug candidates is well described in the literature.^{22–24} Scheme 2 shows the preparation of potential riluzole-derived prodrugs involving conversion of the exocyclic amine to single alpha-amino amides (**4–10**), carbamates (**11–18**), succinamides (**19–23**) and amide linkages from γ -aminobutyric acids (**24, 25**). Plasma bound amidases and esterases would be expected to cleave **4–10** and **11–18**, respectively, to give riluzole directly (Scheme 3, Eqs. 1, 2).²³



Scheme 2. Preparation of riluzole prodrugs. Reagents and conditions (i) RCO_2H , EDCl, DCM; or ROCOCl , Et_3N , DCM; or $\text{RCO}_2\text{COR}'$, DMF, then $\text{R}_1\text{R}_2\text{NH}$, HATU, Et_3N , DMF (ii) TFA, DCM, 2 h if deprotection is required.

Esterases would also act on succinates **20** and **21** and amidases on **22** and **23** to afford resulting acid **19** (Scheme 3, Eq. 4), which would then cyclize to succinic anhydride and riluzole.²⁵ Amines **24** and **25** would release **1** in a pH dependent manner (Scheme 3, Eq. 3),²⁶ and metabolic reduction of *ortho*-nitrophenyl amide analog **26** to the corresponding amino derivative would liberate riluzole as well (Scheme 3, Eq. 5).²⁷

To determine suitability as prodrugs, compounds **4–26** were first tested for stability in various in vitro assays including simulated gastric fluid (SGF), simulated intestinal fluid (SIF), mouse and human liver microsomes (mLM, hLM), as well as mouse and human plasma (mPS, hPS).²⁸ Mouse assays were included to predict in vivo stability for eventual murine xenograft assays. The data are shown graphically in Figure 2.²⁹ Individual assay results indicate disappearance of prodrug, as a percent of the original concentration, after the incubation times indicated. In order to be considered for further study, compounds should be stable in simulated gastric fluid (SGF) and simulated intestinal fluid (SIF) as well as liver microsomes (LM) to predict intact absorption into the plasma. Instability in plasma was assumed to predict in vivo release of the active species required for tumor exposure. Compounds were found to be stable in the SGF assay, however, amino acid derivatives **4–6**, morpholino succinamide **23**, and 4-aminobutyrate analog **25** were rapidly degraded in the SIF assay. Interestingly, γ -aminobutyrate analogue **24** is significantly more stable than substituted aminobutyrate **25**. This stability difference was attributed to the Thorpe-Ingold effect in which the *gem*-dialkyl substitution enhances intramolecular cyclization.³⁰ Stability in the LM assays suggest first pass liver metabolism will be insignificant and systemic exposure will be high.³¹ Hence, derivatives **6, 10, 13, 14, 18–21, 24** and **26** were excluded for further consideration due to instability to LMs. Finally, varying levels of instability were seen with **5, 6, 9** and **20** in the mouse and human plasma assays suggesting the parent substance, riluzole, was being released via plasma amidases.

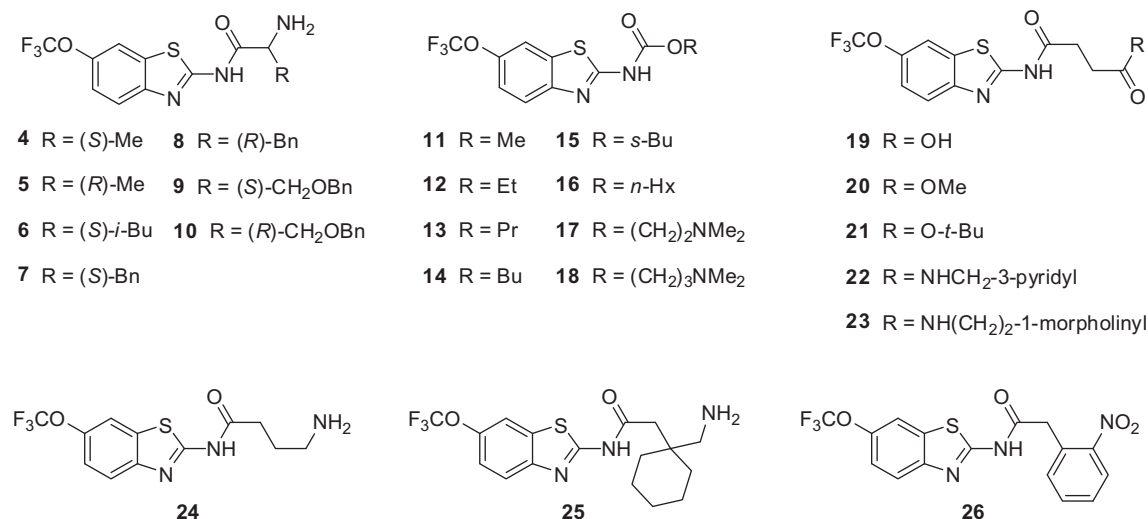
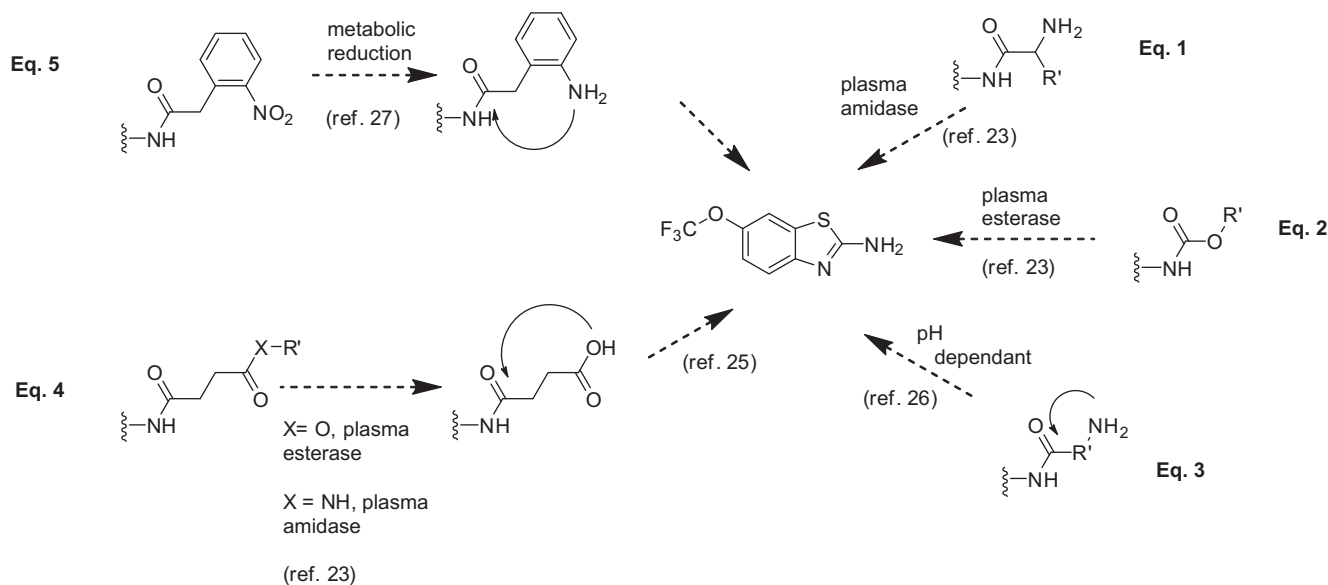


Figure 1. Potential prodrugs of riluzole prepared and evaluated for in vitro stability properties.



Scheme 3. Enzymatic and chemical mechanisms for the release of riluzole from various prodrug classes.

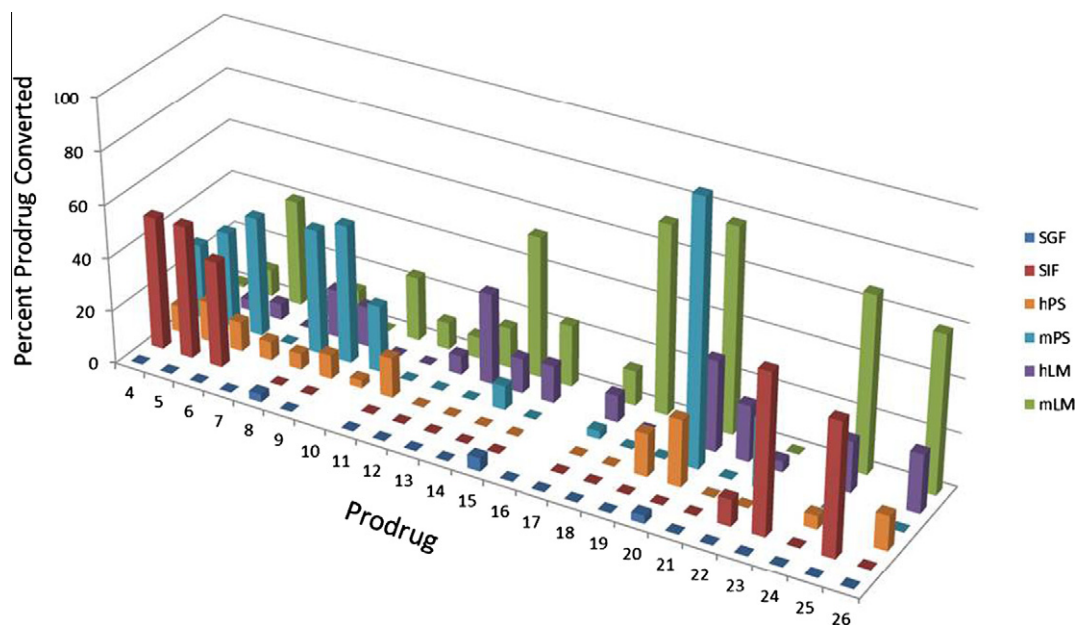


Figure 2. Stability results for potential prodrugs 4–26 evaluated in SGF, SIF, human plasma (*hPS*), mouse plasma (*mPS*), human liver microsomes (*hLM*) and mouse liver microsomes (*mLM*). Vertical bars represent percent disappearance of prodrug after 60 min incubation times (30 min incubation for microsome assays). See Supplementary data for actual data in tabular form. [Intended for color reproduction].

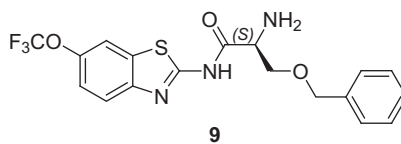
Comparison of all data indicated that **9** had the most promising balance of stability in the intestinal and microsomal assays, and desired lability in the plasma assays. Therefore, this compound was subjected to more extensive analysis to determine half-lives of prodrug disappearance in SGF, SIF, *hLM* and *hPS* assays (Table 1). Riluzole was also detected in the *hPS* assay. The data from these studies support compound **9** as a candidate prodrug that will traverse the GI tract and not be metabolized by the liver.

Riluzole is predominantly metabolized by the CYP1A2 isozyme¹⁹ which is expressed heterogeneously in the population. This leads to variable bioavailability and drug exposure among patients with one report indicating riluzole exposure per kilogram of body weight at 48.7 $\mu\text{g}\cdot\text{h}/\text{L}/\text{Kg}$ with a high standard deviation of 40.9 (189 patients).¹⁸ Before considering prodrug **9** for in vivo

evaluation, we wanted to ensure that this compound itself was not a substrate for oxidative metabolism by CYP1A2 compared to riluzole. Therefore, both riluzole and **9** were subjected to stability assays in liver microsomes from two individual donors expressing high and low CYP1A2 activity, respectively. Microsome baseline activity was determined by disappearance of the CYP1A2 substrate positive control phenacetin accompanied by the appearance of acetaminophen. As expected, riluzole was metabolized to a greater extent in high activity CYP1A2 microsomes (47% remaining at 30 min)²⁰ than in low CYP1A2 activity microsomes (100% remaining at 30 min). Prodrug **9** was not metabolized to a significant extent in either microsome samples with or without the co-factor NADPH ($\geq 70\%$ remaining at 30 min), indicating the prodrug is a poor substrate for the CYP1A2 isozyme (Table 2).

Table 1

Evaluation of compound **9** in various in vitro human stability assays.³² Values are half-lives of prodrug disappearance in the indicated media.



Simulated gastric fluid	Simulated intestinal fluid	Human liver microsomes	Human plasma stability
>60 min	98 min	>60 min	~300 min ^a

^a Riluzole formation occurred during the experiment.

Table 2

Human liver microsome stability of riluzole **1** and prodrug **9** in liver microsomes with high and low Cyp 1A2 activity based on phenacetin metabolism to acetaminophen

Microsomes	NADPH	Time (min)	Riluzole 1 ^a (%)	Compound 9 ^a (%)
High Cyp1A2 Activity ^b	(+)	0	100	100
	(+)	30	47 ^c	70
	(-)	30	100	77
Low Cyp1A2 Activity ^b	(+)	0	100	100
	(+)	30	100	78
	(-)	30	91	76

^a Compounds tested at 1 μ M concentration, $n = 3$.

^b Cyp1A2 activity level was based on 10 fold kinetic conversion ratio of phenacetin to acetaminophen in microsomes.

^c Accompanied by substantial formation of N-hydroxyriluzole.

3. Conclusion

The only FDA-approved drug for ALS, riluzole, has shown promising activity in GRM1 positive melanoma cell assays, refractory melanoma clinical studies and in an in vivo xenograft assay. To stabilize highly variable exposure levels of the drug resulting from patient to patient heterogeneous CYP1A2 expression, putative prodrugs were prepared and evaluated in intestinal, microsome, and plasma stability assays. O-Benzylserine derivative **9** emerged from this process as a preferred prodrug candidate and was further characterized in SGF, SIF, liver microsome, and plasma stability assays. The presence of riluzole was confirmed in the human plasma assay indicating the prodrug is indeed cleaved to provide riluzole. Additional evaluation for metabolism in microsome assays with both high and low CYP1A2 activity levels indicated **9** was most likely not a CYP1A2 substrate. Therefore, compound **9** is expected to be a riluzole prodrug that could display consistent plasma exposure levels upon in vivo administration and is therefore an ideal candidate for testing in murine xenograft efficacy models following evaluation in cell based melanocyte assays, for which data will be reported in due course.

4. Materials and methods

4.1. General

All chemicals and anhydrous solvents were purchased from Sigma–Aldrich (St. Louis, Mo.) and used without additional purification. General solvents and reagents were purchased from Fisher Scientific. ¹H NMR spectra were obtained on a Varian Mercury 300-MHz NMR. Purity (%) and mass spectral data were determined with a Waters Alliance 2695 HPLC/MS (Waters Symmetry C18, 4.6 \times 75 mm, 3.5 μ m) with a 2996 diode array detector from 210–400 nm; the solvent system is 5–95% MeCN in water over nine mins using a linear gradient and retention times are in minutes. Yields refer to the amount of product after purification and are not optimized.

4.2. General synthetic method of amide analogs **4–10**, **24–26**

6-Trifluoromethoxy-benzothiazol-2-ylamine (**1**, 100 mg, 0.42 mmol), a carboxylic acid (0.43 mmol), and EDCI (123 mg, 0.65 mmol) were combined in methylene chloride (5 mL) and stirred 4 days. The reaction was washed with 0.1 N HCl (2 \times 10 mL), dried over magnesium sulfate, filtered, and then concentrated. Chromatography on silica gel afforded the *t*-Boc protected compounds as well as compound **26** directly. Compounds **4–10**, **24**, and **25** were dissolved in 4 N HCl and 1,4-dioxane and stirred 3 h at ambient temperature. The reactions were then concentrated to afford the products.

4.3. (S)-2-Amino-N-(6-trifluoromethoxybenzothiazol-2-yl)-propionamide (**4**)

Yield: 71%; white powder. ¹H NMR (300 MHz, DMSO-*d*₆) δ 8.57 (s, 1H), 8.18 (s, 1H), 7.88 (d, $J = 8.8$ Hz, 1H), 7.46 (d, $J = 8.8$ Hz, 1H), 4.78–3.63 (m, 1H), 1.46 (d, $J = 7.1$ Hz, 3H). HPLC–MS m/z (M^+) 305.9; $T_r = 3.58$ (95%).

4.4. (R)-2-Amino-N-(6-trifluoromethoxybenzothiazol-2-yl)-propionamide (**5**)

Yield: 59%; white powder. ¹H NMR (300 MHz, DMSO) δ 8.57 (s, 1H), 8.18 (s, 1H), 7.88 (d, $J = 8.8$ Hz, 1H), 7.46 (d, $J = 8.8$ Hz, 1H), 3.98 (bs, 3H), 1.46 (d, $J = 7.1$ Hz, 3H). HPLC–MS m/z (M^+) 305.9; $T_r = 3.57$ (>95%).

4.5. (S)-2-Amino-3-methyl-N-(6-trifluoromethoxybenzothiazol-2-yl)-butyramide (**6**)

Yield: 66%; white powder. ¹H NMR (300 MHz, DMSO-*d*₆) δ 8.55 (s, 1H), 8.18 (s, 1H), 7.88 (d, $J = 8.8$ Hz, 1H), 7.46 (d, $J = 8.9$ Hz, 1H), 4.00 (m, 1H), 3.43 (m, 2H), 3.16 (s, 4H), 2.26 (d, $J = 6.4$ Hz, 1H), 1.29–0.63 (m, 6H). HPLC–MS m/z (M^+) 333.9; $T_r = 3.92$ (>95%).

4.6. (S)-2-Amino-3-phenyl-N-(6-trifluoromethoxybenzothiazol-2-yl)-propionamide (7)

Yield: 83%; beige powder. ¹H NMR (300 MHz, CD₃OD) δ 7.90 (s, 1H), 8.05–7.47 (m, 2H), 7.81 (d, *J* = 8.9 Hz, 1H), 7.34 (dt, *J* = 9.7, 7.8 Hz, 2H), 7.34 (dt, *J* = 9.7, 7.8 Hz, 2H), 4.40 (dd, *J* = 8.1, 6.3 Hz, 1H), 3.46–3.30 (m, 2H), 3.19 (dd, *J* = 14.0, 8.2 Hz, 1H). HPLC–MS *m/z* (M⁺) 381.9; *T_r* = 4.27 (>95%).

4.7. (R)-2-Amino-3-phenyl-N-(6-trifluoromethoxybenzothiazol-2-yl)-propionamide (8)

Yield: 72%; white powder. ¹H NMR (300 MHz, DMSO-*d*₆) δ 8.75 (bs, 2H), 8.31 (s, 1H), 7.99 (d, *J* = 8.9 Hz, 1H), 7.59 (d, *J* = 8.8 Hz, 1H), 7.42 (m, 4H), 4.53 (bs, 1H), 3.44 (s, 2H), 3.32 (m, 2H). HPLC–MS *m/z* (M⁺) 381.9; *T_r* = 4.21 (>95%).

4.8. (S)-2-Amino-3-benzyloxy-N-(6-trifluoromethoxybenzothiazol-2-yl)-propionamide (9)

Yield: 66%; white powder. ¹H NMR (300 MHz, DMSO-*d*₆) δ 8.66 (s, 1H), 8.19 (s, 1H), 7.88 (d, *J* = 8.9 Hz, 1H), 7.47 (d, *J* = 8.9 Hz, 1H), 7.35–7.18 (m, 5H), 4.56 (q, *J* = 12.3 Hz, 2H), 4.44 (s, 1H), 4.11–3.77 (m, 2H). HPLC–MS *m/z* (M⁺) 411.9; *T_r* = 4.40 (95%).

4.9. (R)-2-Amino-3-benzyloxy-N-(6-trifluoromethoxybenzothiazol-2-yl)-propionamide (10)

Yield: 48%; buff powder. ¹H NMR (300 MHz, DMSO-*d*₆) δ 8.37 (d, *J* = 103.5 Hz, 1H), 8.20 (s, 1H), 7.89 (d, *J* = 8.8 Hz, 1H), 7.48 (d, *J* = 9.6 Hz, 1H), 7.40–7.18 (m, 5H), 4.57 (q, *J* = 12.4 Hz, 2H), 4.42 (m, 2H), 4.06–3.82 (m, 1H), 3.50 (s, 1H). HPLC–MS *m/z* (M⁺) 411.9; *T_r* = 4.43 (>95%).

4.10. 5-Aminopentanoic acid (6-trifluoromethoxybenzothiazol-2-yl)-amide (24)

Yield: 77%; white powder. ¹H NMR (300 MHz, CD₃OD) δ 8.00–7.65 (m, 2H), 7.34 (d, *J* = 8.9 Hz, 1H), 3.72 (t, *J* = 6.6 Hz, 2H), 3.2–2.89 (m, 2H), 2.71 (t, *J* = 7.0 Hz, 2H), 2.17–1.93 (m, 2H), 1.93–1.73 (m, 2H). MS *m/z* (M+Na⁺) 342.0; *T_r* = 3.45 (>95%).

4.11. 2-(1-Aminomethyl-cyclohexyl)-N-(6-trifluoromethoxybenzothiazol-2-yl)-acetamide (25)

Yield: 34%; buff powder. ¹H NMR (300 MHz, DMSO-*d*₆) δ 12.70 (s, 1H), 8.88 (s, 1H), 8.14 (s, 1H), 7.97 (s, 1H), 7.85 (d, *J* = 8.8 Hz, 1H), 7.44 (d, *J* = 8.8 Hz, 1H), 3.01 (d, *J* = 5.6 Hz, 4H), 2.90 (s, 3H), 2.80 (s, 3H), 2.74 (s, 3H), 1.47 (d, *J* = 8.8 Hz, 3H). MS *m/z* (MH⁺) 388.0; *T_r* = 4.03 (96%).

4.12. 2-(2-Nitrophenyl)-N-(6-trifluoromethoxybenzothiazol-2-yl)-acetamide (26)

Yield: 38%; white powder. ¹H NMR (300 MHz, DMSO-*d*₆) δ 12.79 (s, 1H), 8.12 (d, *J* = 8.2 Hz, 2H), 7.84 (d, *J* = 8.8 Hz, 1H), 7.75 (d, *J* = 7.4 Hz, 1H), 7.62 (d, *J* = 5.6 Hz, 2H), 7.42 (d, *J* = 8.7 Hz, 1H), 4.30 (s, 2H). MS *m/z* (M⁺) 397.9; *T_r* = 5.77 (>95%).

4.13. General synthetic method for carbamate analogs 11–18

6-Trifluoromethoxybenzothiazol-2-ylamine (**1**, 100 mg, 0.42 mmol), chloroformate (0.74 mmol), and triethylamine (64 mg, 0.64 mmol) were combined in methylene chloride (3 mL) and stirred 24 h at ambient temperature. The reaction was concentrated. The residue was treated with methanol/water (1:1, 5 mL) and the

solid collected by filtration and dried under vacuum to afford product.

4.14. (6-Trifluoromethoxybenzothiazol-2-yl)-carbamic acid methyl ester (11)

Yield: 47%; white powder. ¹H NMR (300 MHz, DMSO-*d*₆) δ 8.22 (s, 1H), 7.89 (d, *J* = 8.8 Hz, 1H), 7.52 (d, *J* = 9.0 Hz, 1H), 3.97 (s, 1H), 3.44 (s, 3H). HPLC–MS *m/z* (M⁺) 292.9; *T_r* = 5.26 (94%).

4.15. (6-Trifluoromethoxybenzothiazol-2-yl)-carbamic acid ethyl ester (12)

Yield: 67%; white powder. ¹H NMR (300 MHz, DMSO-*d*₆) δ 8.23 (s, 1H), 7.90 (d, *J* = 8.8 Hz, 1H), 7.52 (d, *J* = 8.7 Hz, 1H), 4.40 (q, *J* = 7.1 Hz, 2H), 1.42 (t, *J* = 7.1 Hz, 3H). HPLC–MS *m/z* (M⁺) 306.9; *T_r* = 5.62 (96%).

4.16. (6-Trifluoromethoxybenzothiazol-2-yl)-carbamic acid propyl ester (13)

Yield: 74%; white powder. ¹H NMR (300 MHz, DMSO-*d*₆) δ 12.15 (s, 1H), 8.10 (s, 1H), 7.77 (d, *J* = 8.8 Hz, 1H), 7.39 (d, *J* = 8.6 Hz, 1H), 4.18 (t, *J* = 6.7 Hz, 2H), 2.57–2.45 (m, 2H), 0.95 (t, *J* = 7.4 Hz, 3H). HPLC–MS *m/z* (M⁺) 320.9; *T_r* = 5.98 (95%).

4.17. (6-Trifluoromethoxybenzothiazol-2-yl)-carbamic acid butyl ester (14)

Yield: 56%; white powder. ¹H NMR (300 MHz, DMSO-*d*₆) δ 12.14 (s, 1H), 8.09 (s, 1H), 7.77 (d, *J* = 8.8 Hz, 1H), 7.39 (d, *J* = 7.4 Hz, 1H), 4.21 (t, *J* = 6.7 Hz, 1H), 1.73–1.31 (m, 2H), 1.32 (t, *J* = 6.9 Hz, 2H), 0.88 (t, *J* = 6.7 Hz, 3H). HPLC–MS *m/z* (M⁺) 334.9; *T_r* = 6.36 (95%).

4.18. (6-Trifluoromethoxybenzothiazol-2-yl)-carbamic acid isobutyl ester (15)

Yield: 66%; white powder. ¹H NMR (300 MHz, DMSO-*d*₆) δ 12.16 (s, 1H), 8.08 (s, 1H), 7.76 (d, *J* = 8.8 Hz, 1H), 7.38 (d, *J* = 7.2 Hz, 1H), 3.97 (dd, *J* = 18.1, 6.6 Hz, 2H), 1.96 (dt, *J* = 13.5, 6.8 Hz, 1H), 1.05 (d, *J* = 6.6 Hz, 3H). HPLC–MS *m/z* (M⁺) 334.9; *T_r* = 6.33 (>95%).

4.19. (6-Trifluoromethoxybenzothiazol-2-yl)-carbamic acid hexyl ester (16)

Yield: 72%; white powder. ¹H NMR (300 MHz, DMSO-*d*₆) δ 8.12 (s, 1H), 7.79 (d, *J* = 8.8 Hz, 1H), 7.42 (d, *J* = 7.4 Hz, 1H), 4.24 (t, *J* = 6.7 Hz, 2H), 1.67 (dd, *J* = 14.2, 6.8 Hz, 2H), 1.35 (m, 6H), 0.91 (t, *J* = 6.7 Hz, 3H). HPLC–MS *m/z* (M⁺) 362.9; *T_r* = 6.97 (95%).

4.20. (6-Trifluoromethoxybenzothiazol-2-yl)-carbamic acid 2-dimethylamino-ethyl ester (17)

Yield: 13%; white powder. ¹H NMR (300 MHz, CD₃OD) δ 7.85 (s, 1H), 7.75 (d, *J* = 9.1 Hz, 1H), 7.42–7.27 (m, 1H), 4.86 (s, 6H), 4.64 (m, 2H), 3.58 (m, 2H). HPLC–MS *m/z* (M⁺) 349.8; *T_r* = 3.58 (>95%).

4.21. (6-Trifluoromethoxybenzothiazol-2-yl)-carbamic acid 3-(dimethylamino)propyl ester (18)

Yield: 14%; beige powder. ¹H NMR (300 MHz, DMSO-*d*₆) δ 10.33 (s, 1H), 8.10 (s, 1H), 7.77 (d, *J* = 8.8 Hz, 1H), 7.39 (d, *J* = 8.7 Hz, 1H), 4.26 (dd, *J* = 18.9, 12.6 Hz, 2H), 3.16 (d, *J* = 15.6 Hz, 2H), 2.76 (d, *J* = 5.0 Hz, 6H), 2.30–1.77 (m, 2H). HPLC–MS *m/z* (M⁺) 363.9; *T_r* = 3.71 (>95%).

4.22. General synthesis method of amide analogs 19–21

6-Trifluoromethoxy-benzothiazol-2-ylamine (**1**, 100 mg, 0.42 mmol), a carboxylic acid (0.43 mmol), and EDCI (123 mg, 0.65 mmol) were combined in methylene chloride (5 mL) and stirred 4 days. The reaction was washed with 0.1 N HCl (2 × 10 mL), dried over magnesium sulfate, filtered, and then concentrated. Chromatography on silica gel afforded compounds **20**, and **21**. Compound **21** was dissolved in dichloromethane and trifluoroacetic acid (1:1). After stirring 2 h the solvents were removed in vacuo to yield compound **19**.

4.23. N-(6-Trifluoromethoxybenzothiazol-2-yl)-succinamic acid (**19**)

Yield: 71%; white powder. $^1\text{H NMR}$ (300 MHz, DMSO- d_6) δ 8.11 (s, 1H), 7.81 (d, J = 8.8 Hz, 1H), 7.41 (d, J = 8.8 Hz, 1H), 2.72 (d, J = 6.8 Hz, 2H), 2.68–2.44 (m, 2H). HPLC–MS m/z (M^+) 334.8; T_r = 4.60 (>95%).

4.24. N-(6-Trifluoromethoxybenzothiazol-2-yl)-succinamic acid methyl ester (**20**)

Yield: 77%; white powder. $^1\text{H NMR}$ (300 MHz, DMSO- d_6) δ 12.54 (s, 2H), 8.12 (s, 1H), 7.82 (d, J = 8.8 Hz, 1H), 7.42 (d, J = 8.8 Hz, 1H), 3.60 (d, J = 9.2 Hz, 3H), 3.03–2.58 (m, 2H), 1.76 (t, J = 6.6 Hz, 2H). HPLC–MS m/z (M^+) 348.9; T_r = 5.23 (>95%).

4.25. N-(6-Trifluoromethoxybenzothiazol-2-yl)-succinamic acid tert-butyl ester (**21**)

Yield: 33%; light yellow powder. $^1\text{H NMR}$ (300 MHz, DMSO- d_6) δ 12.50 (s, 1H), 8.10 (s, 1H), 7.81 (d, J = 8.6 Hz, 1H), 7.40 (m, 1H), 3.59 (t, J = 6.6 Hz, 2H), 1.75 (t, J = 6.6 Hz, 2H), 1.37 (s, 9H). HPLC–MS m/z (M^+ - C_4H_9) 334.8; T_r = 6.08 (95%).

4.26. Synthesis of amide analogs 22 and 23

Maleic anhydride (1 mmol) and an amine (1 mmol) were stirred in DMF (1 mL) 24 h. 6-Trifluoromethoxy-benzothiazol-2-ylamine (**1**, 1 mmol), HATU (1 mmol), and Et₃N (1 mmol) were the reaction was stirred an additional 24 h. The reactions were purified using reverse phase chromatography to afford the desired compounds.

4.27. N-Pyridin-3-ylmethyl-N'-(6-trifluoromethoxybenzothiazol-2-yl)-succinamide (**22**)

Yield: 16%; beige powder. $^1\text{H NMR}$ (300 MHz, DMSO- d_6) δ 12.50 (s, 1H), 8.84–8.42 (m, 2H), 8.10 (d, J = 7.4 Hz, 2H), 7.81 (d, J = 8.8 Hz, 2H), 7.71 (d, J = 7.9 Hz, 1H), 7.35 (dd, J = 36.7, 27.4 Hz, 1H), 4.40 (d, J = 5.8 Hz, 2H), 2.78 (t, J = 6.7 Hz, 2H), 2.57 (t, J = 6.7 Hz, 2H). HPLC–MS m/z (M^+) 424.9; T_r = 3.49 (95%).

4.28. N-(2-Morpholin-4-yl-ethyl)-N'-(6-trifluoromethoxybenzothiazol-2-yl)-succinamide (**23**)

Yield: 9%; white powder. $^1\text{H NMR}$ (300 MHz, DMSO- d_6) δ 12.51 (s, 1H), 9.61 (s, 1H), 8.23 (s, 1H), 8.11 (s, 1H), 7.82 (d, J = 8.9 Hz, 1H), 7.42 (d, J = 8.9 Hz, 1H), 3.96 (s, 2H), 3.64 (s, 3H), 3.44 (m, 6H), 3.18 (m, 3H), 2.76 (d, J = 6.4 Hz, 2H), 2.53 (dd, J = 15.1, 4.8 Hz, 1H). MS m/z (M^+) 446.9; T_r = 3.66 (95%).

5. In vitro stability assays

5.1. Stability in Simulated Gastric Fluid (SGF) and Simulated Intestinal Fluid (SIF)

The compounds were prepared in a 9:1 mixture of the appropriate test component (SGF, SIF) and acetonitrile to a final

concentration of 0.01 mg/mL. The samples were thoroughly mixed and maintained at 37 °C for 60 min. Each sample was injected consecutively onto an Agilent 1100 system (Luna C18, 3 μm , 50 mm × 3 mm; 1 mL/min; mobile phase of 0.1% trifluoroacetic acid in water/0.1% trifluoroacetic acid in acetonitrile) after a 60 min period. The percent prodrug conversion was calculated by comparing the area of prodrug compound versus riluzole generated. The identities of the parent compounds and conversion products were confirmed by LC/MS.

5.2. Plasma stability

Assessment of plasma stability was carried out by individual incubations of drug candidates in fresh mouse or human control plasma at a concentration of 1 μM for 1 h at 37 °C. After which, the samples were de-proteinized by addition of 2 volumes of acetonitrile containing 0.1% formic acid and internal standard, vortex mixed for 2 min and centrifuged at 4000 rpm for 10 min to pellet precipitated protein. The resulting supernatants containing the drug candidates were diluted fivefold with water containing 0.1% formic acid and submitted to LC–MS/MS analysis. All determinations were done in triplicate. Plasma stability was expressed as percent of control remaining.

5.3. Metabolic stability

In vitro metabolic stability was determined in pooled mouse or human liver microsomes (BD Gentest) at a protein concentration of 0.5 mg/mL in reaction buffer (100 mM KH₂PO₄, pH 7.4 and 12 mM MgCl₂). Each drug candidate was added to a final concentration of 1 μM . This mixture was pre-warmed to 37 °C for 10 min prior to starting the reaction with the addition of β -nicotinamide adenine dinucleotide 2'-phosphate reduced (NADPH) to a final concentration of 1 mM. A parallel incubation lacking NADPH served as the control. After incubation for 30 min at 37 °C, the reactions were quenched by the addition of acetonitrile containing 0.1% formic acid and internal standard, vortex mixed for 2 min and centrifuged at 4000 rpm for 10 min to pellet the precipitated protein. The resulting supernatant containing the drug candidate and its potential metabolites was diluted fivefold with water containing 0.1% formic acid and submitted to LC/MS/MS analysis. Metabolic stability was expressed as percent of control remaining.

5.4. Cyp1A2 metabolic stability

Microsomes were purchased from Invitrogen as frozen 20 mg/mL solutions. Two individual donor microsome lots were used which had a wide range of Cyp1A2 activity as measured by Invitrogen using a phenacetin dealkylation activity assay. Lot# HU8045 was determined to have a V_{max} for the demethylation of phenacetin of 94.7 $\mu\text{mol}/\text{min}$ and Lot# HU8022 was determined to have a V_{max} of 1190 $\mu\text{mol}/\text{min}$. Individual microsome lots were used to determine the metabolic disappearance of Riluzole and Riluzole prodrug **9** using the incubation method from the **Metabolic Stability** section above.

5.5. LC–MS/MS analysis

An aliquot from each incubation was analyzed by LC/MS/MS with SRM detection in the positive ionization mode using an ABSciex API 5500 QTrap Mass Spectrometer interfaced via the ABSciex Turbo V IonSpray source (ESI) to an Eksigent ExpressHT LC system. Best peak shape and separation from interfering matrix species was afforded by an Eksigent 3C18-CL-300, 3 μm , 50 × 1 mm column.

A fast gradient, from 15 to 85% organic in 2.5 min, with run time of 5.0 min, and flow rate of 50 $\mu\text{L}/\text{min}$ was utilized. Peak areas were integrated using MultiQuant v2.0 software from ABSciex.

Acknowledgments

This work was funded by a Grant from the National Cancer Institute of the National Institutes of Health (R43 CA156781-01).

Supplementary data

Supplementary data associated with this article can be found, in the online version, at <http://dx.doi.org/10.1016/j.bmc.2012.07.004>.

References and notes

1. Cavaleiro, E. A.; Olney, J. W. *Proc. Natl. Acad. Sci. USA* **2001**, *98*, 5947.
2. Takano, T.; Lin, J. H.; Arcuino, G.; Gao, Q.; Yang, J.; Nedergaard, M. *Nat. Med.* **2001**, *7*, 1010.
3. Kalariti, N.; Pissimissis, N.; Koutsilieris, M. *Expert Opin. Investig. Drugs* **2005**, *14*, 1487.
4. Ackermann, J.; Beermann, F. *Pigment Cell Res.* **2005**, *18*, 315.
5. Rzeski, W.; Ikonomidou, C.; Turski, L. *Biochem. Pharmacol.* **2002**, *64*, 1195.
6. Rzeski, W.; Turski, L.; Ikonomidou, C. *Proc. Natl. Acad. Sci. USA* **2001**, *98*, 6372.
7. Stepulak, A.; Siffringer, M.; Rzeski, W., et al *Proc. Natl. Acad. Sci. USA* **2005**, *102*, 15605.
8. Doble, A. *Neurology* **1996**, *47*, 2335.
9. Kretschmer, B. D.; Kratzer, U.; Schmidt, W. J. *Naunyn-Schmiedeberg's Arch Pharmacol.* **1998**, *358*, 181.
10. Wang, S. J.; Wang, K. Y.; Wang, W. C. *Neuroscience* **2004**, *125*, 191.
11. Namkoong, J.; Shin, S. S.; Lee, H. J., et al *Cancer Res.* **2007**, *67*, 2298.
12. Shuff, J. H.; Siker, M. L.; Daly, M. D.; Schultz, C. J. *Clin. Plas. Surg.* **2010**, *37*, 147.
13. Trinh, V. A. *Am. J. Health Syst. Pharm.* **2008**, *65*, 3.
14. Sondak, V. K.; Flaherty, L. E. *Nat. Rev. Clin. Oncol.* **2011**, *8*, 513.
15. Luke, J. J.; Hodi, F. S. *Clin. Cancer Res.* **2012**, *18*, 9.
16. Bensimon, G.; Lacomblez, L.; Meiningner, V. N. *Engl. J. Med.* **1994**, *330*, 585.
17. Yip, D.; Le, M. N.; Chan, J. L.-K.; Lee, J. H.; Mehnert, J. A.; Yudd, A.; Kempf, J.; Shih, W. J.; Chen, S.; Goydos, J. S. *Clin. Cancer Res.* **2009**, *15*, 3896.
18. Groeneveld, G. J.; Van Kan, H. J. M.; Kalmijn, S., et al *Neurology* **2003**, *61*, 1141.
19. van Kan, H. J. M.; Groeneveld, G. J.; Kalmijn, S.; Spijksma, M.; van den Berg, L. H.; Guchelaar, H. J. *Brit. J. Clin. Pharmacol.* **2004**, *59*, 310.
20. Sanderink, G. J.; Bournique, B.; Stevens, J.; Petry, M.; Martinet, M. *J. Pharmacol. Exp. Ther.* **1997**, *282*, 1465.
21. Martinet, M.; Montay, G.; Rhodes, G. *Drugs Today* **1997**, *33*, 587.
22. Ettmayer, P.; Amidon, G. L.; Clement, B.; Testa, B. *J. Med. Chem.* **2004**, *47*, 2393.
23. Rautio, J.; Kumpulainen, H.; Heimbach, T., et al *Nat. Rev. Drug Disc.* **2008**, *7*, 255.
24. Testa, B. *Biochem. Pharmacol.* **2004**, *68*, 2097.
25. Fredholt, K.; Mork, N.; Begtrup, M. *Int. J. Pharm.* **1995**, *123*, 209.
26. Nam, N.-H.; Kim, Y.; You, Y.-J.; Hong, D.-H.; Kim, H.-M.; Ahn, B.-Z. *Bioorg. Med. Chem.* **2003**, *11*, 1021.
27. Sykes, B. M.; Atwell, G. J.; Hogg, A.; Wilson, W. R.; O'Connor, C. J.; Denny, W. A. *J. Med. Chem.* **1999**, *42*, 346.
28. Di, L.; Kerns, E. H. *Curr. Opin. Drug Disc. Devel.* **2005**, *8*, 495.
29. Baudy, R. B.; Butera, J. A.; Abou-Gharbia, M. A.; Chen, H.; Harrison, B.; Jain, U.; Magolda, R.; Sze, J. Y.; Brandt, M. R.; Cummons, T. A.; Kowal, D.; Pangalos, M. N.; Zupan, B.; Hoffmann, U. M.; May, M.; Mugford, C.; Kennedy, J.; Childers, W. E., Jr. *J. Med. Chem.* **2009**, *52*, 771.
30. Jung, M. E.; Piizzi, G. *Chem. Rev.* **2005**, *105*, 1735.
31. Mandagere, A. K.; Thompson, T. N.; Hwang, K.-K. *J. Med. Chem.* **2002**, *45*, 304.
32. Assays performed by Absorption Systems, Inc. Exton, PA.